Cell Reports, Volume *37*

Supplemental information

ILC3s control airway inflammation by limiting T cell responses to allergens and microbes

Fei Teng, Roser Tachó-Piñot, Biin Sung, Donna L. Farber, Stefan Worgall, Hamida Hammad, Bart N. Lambrecht, Matthew R. Hepworth, and Gregory F. Sonnenberg

Figure S1

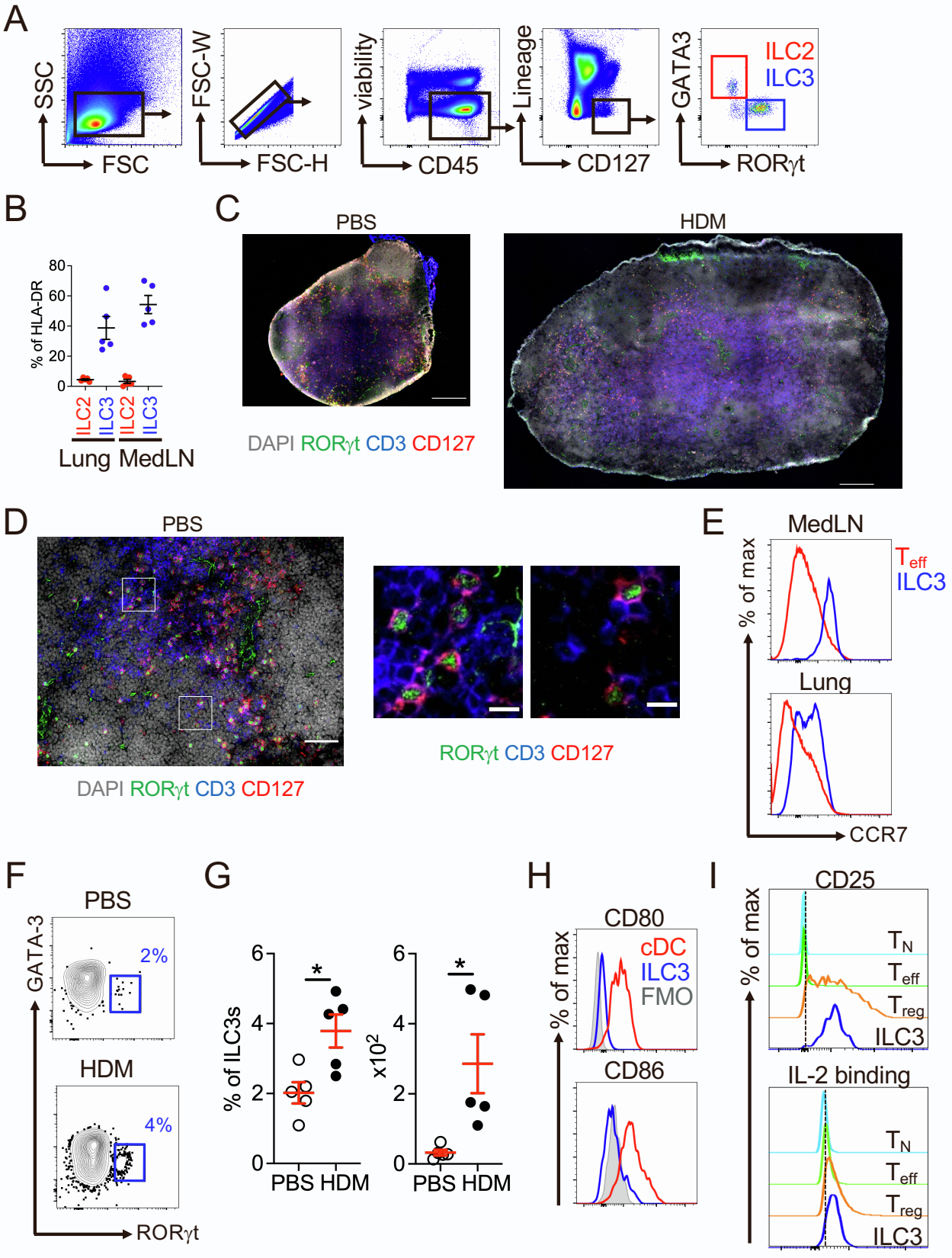
A
SSC
FSC
FSC-W
FSC-H
viability
CD45
Lineage
CD127
GATA3
RORγt
ILC2
ILC3
B
% of HLA-DR
80
60
40
20
0
ILC2
ILC3
ILC2
ILC3
Lung
MedLN
C
PBS
HDM
DAPI RORγt CD3 CD127
D
PBS
DAPI RORγt CD3 CD127
RORγt CD3 CD127
E
MedLN
% of max
Teff
ILC3
Lung
CCR7
F
PBS
GATA-3
2%
HDM
4%
RORγt
G
% of ILC3s
6
4
2
0
*
PBS HDM
x10²
6
4
2
0
*
PBS HDM
H
CD80
% of max
cDC
ILC3
FMO
CD86
I
CD25
% of max
TN
Teff
Treg
ILC3
IL-2 binding
TN
Teff
Treg
ILC3

Figure S1. Defining ILC3 in the airway draining lymph nodes, related to Figure 1. (A) Representative gating strategy for ILC2s and ILC3s. (B) Quantitative bar graphs of the frequency of HLA-DR$^+$ ILC2s and ILC3s in human lung and MedLN tissues. Data are from 5 individual donors. (C) Representative immunofluorescence staining for ILC3s and T cells of whole MedLN of mice exposed to PBS or HDM. Scale bar = 200 μm. (D) Representative images (Scale bar = 50 μm; left panel) and highlighted inserts (Scale bar = 10 μm; right panel) showing ILC3 and T cells in the MedLN of PBS exposed mice (representative of 2 independent assays, *n=3* mice per group). Representative staining of CCR7 (E), ILC3s (F) and quantitative bar graphs of ILC3s (G) from lung parenchyma or MedLN of B6 WT mice after exposure to HDM or PBS (data pooled from 5 mice per group). Effector T cells were gated as CD44$^+$CD62L$^-$. (H) Representative staining of CD80 and CD86 on ILC3s versus cDCs in the MedLN of PBS exposed mice. (I) Representative histograms of CD25 and IL-2 binding on gated cell populations in the MedLN following exposure to HDM (and quantified in Figure 2C). Data are represented as mean ± SEM. Statistics are calculated by Student's t-test.

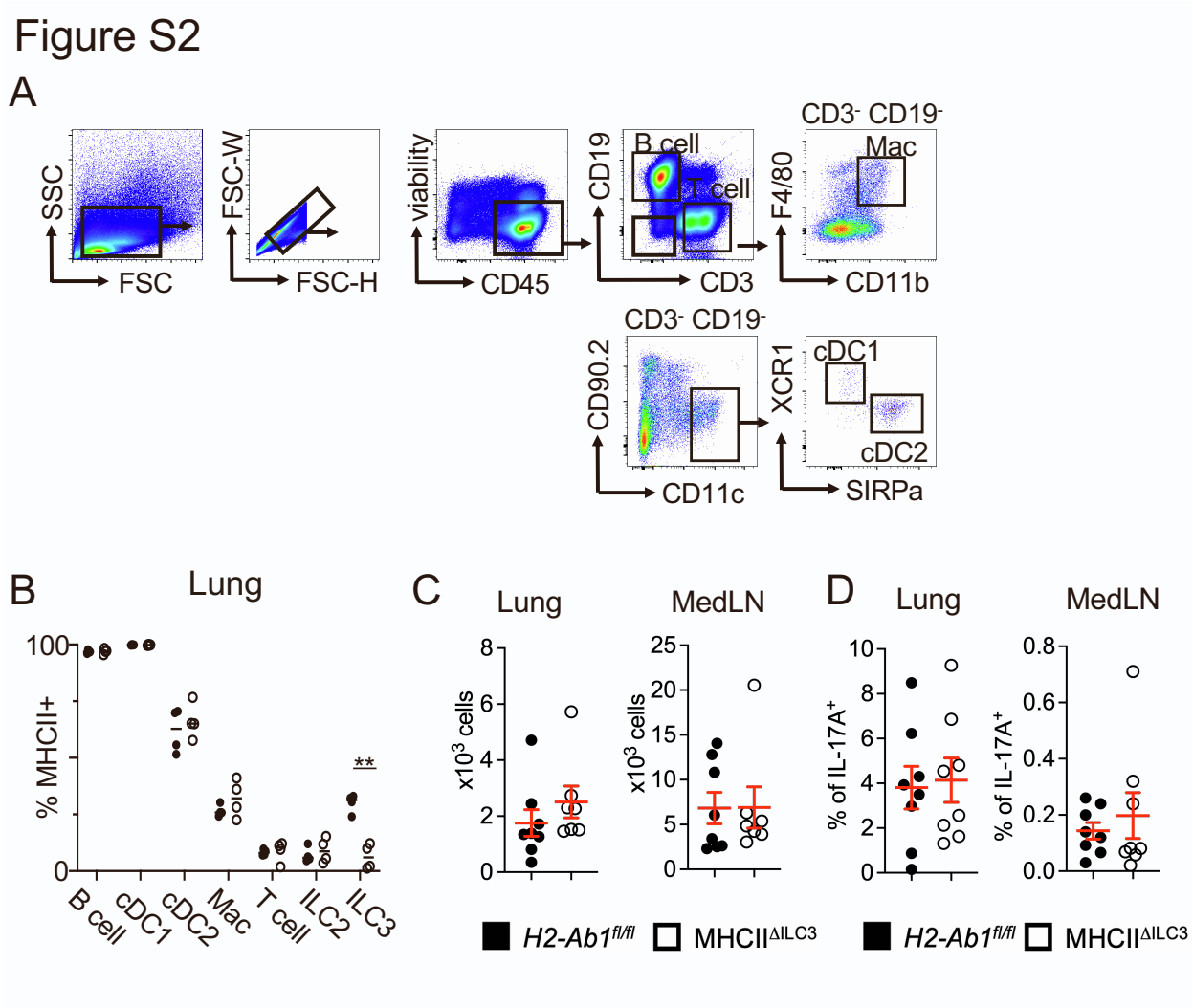

Figure S2. Selective targeting of ILC3-specific MHCII, related to Figure 2. (A) Representative gating of myeloid cells and lymphocytes and (B) quantification of MHCII on those cell types in the HDM-exposed lung parenchyma (data representative of two independent experiments, n = 4). Quantitative bar graphs of the total cell number (C) or frequency of IL-17A$^+$ (D) CD45.1$^+$ donor DerP1-specific TCR transgenic CD4$^+$ T cells in lung parenchyma and MedLN from recipient *H2-Ab1$^{fl/fl}$* and MHCII$^{\Delta ILC3}$ mice after exposure to HDM. Cells were gated on live CD45$^+$ CD19$^-$ TCRβ$^+$ CD4$^+$ (data pooled from 2 independent assays, n = 7-8). Data are represented as mean ± SEM. Statistics are calculated by two-way ANOVA (B) and Student's t-test (C and D).

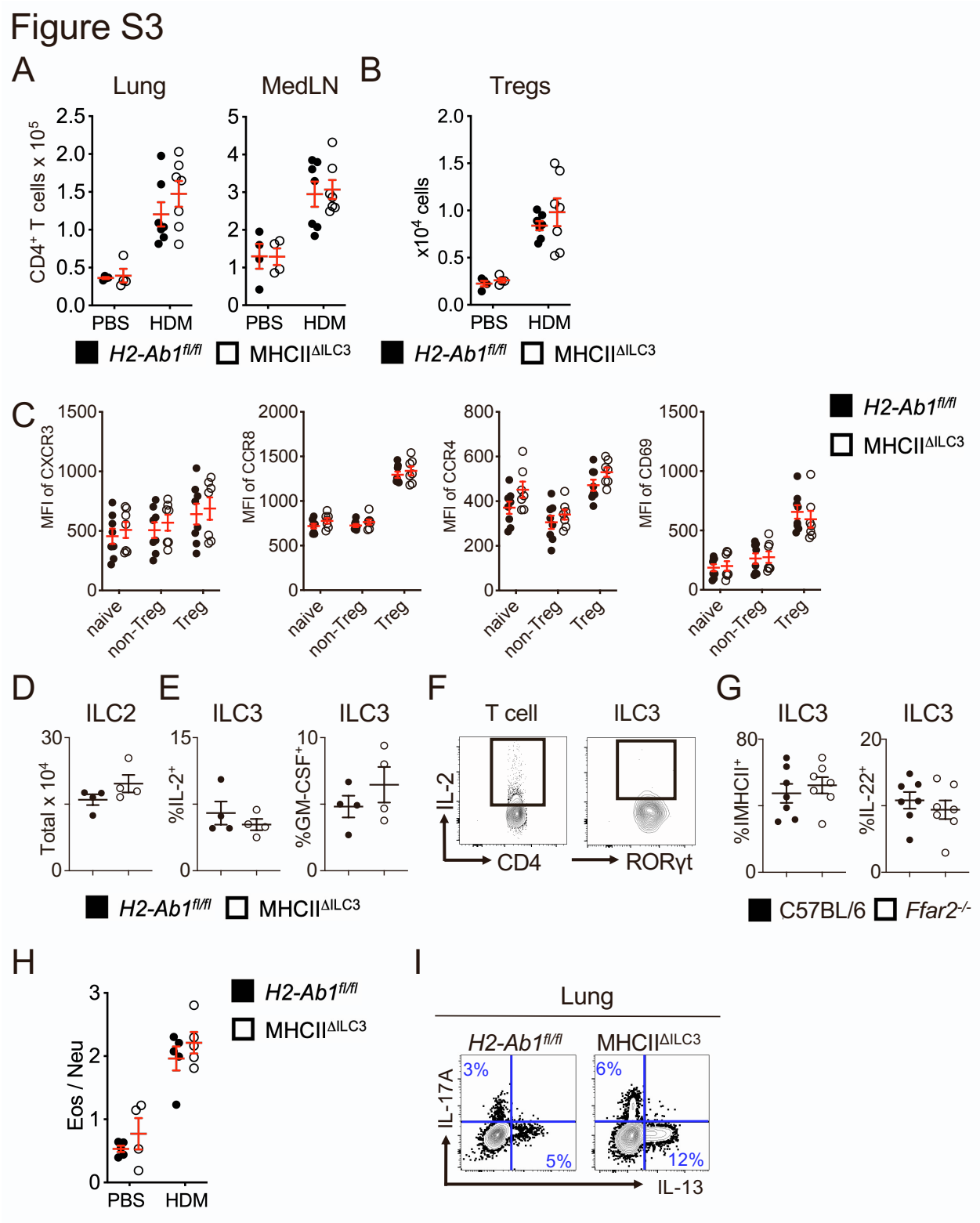

Figure S3. ILC3-specific MHCII does not impact other ILC effector programs or T cell homing receptors, related to Figure 3. *H2-Ab1*$^{fl/fl}$ and MHCII$^{\Delta ILC3}$ mice were exposed to HDM and quantified for (A) total lung CD4$^+$ T cells, (B) lung Tregs, (C) designated homing receptors on lung T cells, (D) ILC2 numbers in the lung, and (E) frequencies of IL-2$^+$ and GM-CSF$^+$ ILC3s in the MedLN (data are representative from 2 independent assays, n = 4-

7). (F) Representative staining of IL-2^{+} T cells and ILC3s in the MedLN as quantified in (E). (G) C57BL/6 and *Ffar2*$^{-/-}$ mice were exposed to HDM and quantified for MHCII^{+} or IL-22^{+} ILC3s in the MedLN data are representative from 2 independent assays, n = 7). *H2-Ab1*$^{fl/fl}$ and MHCII$^{\Delta ILC3}$ mice were exposed to HDM and quantified for (H) eosinophil/neutrophil ratios in the lung, and (I) **r**epresentative plots of IL-17A and IL-13 cytokine expression in lung CD4^{+} T cells (representative from at least 2 independent assays, n = 5). Data are represented as mean ± SEM.

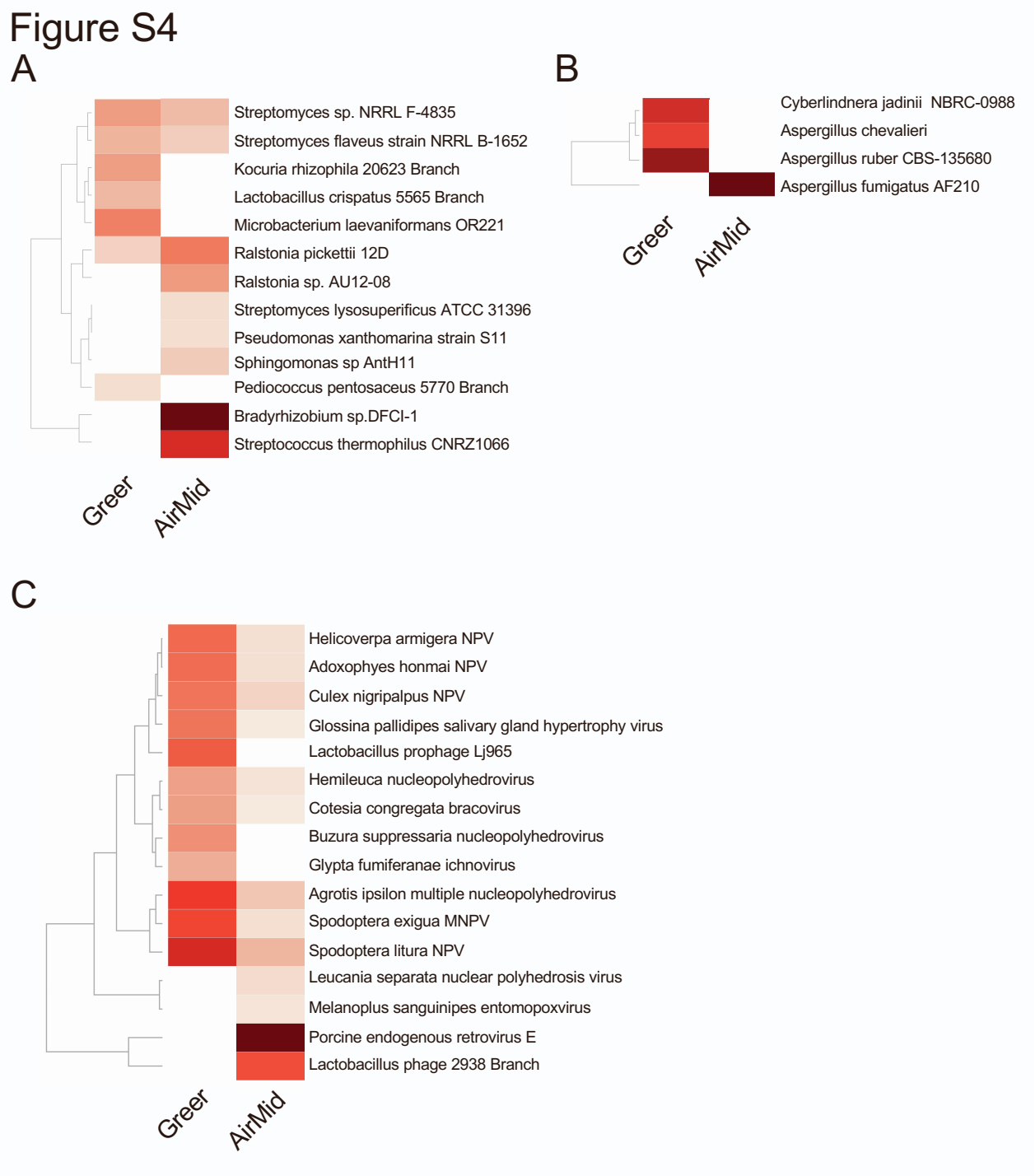

Figure S4. Different composition of microbial community between Greer and AirMid sourced HDM, related to Figure 4. Heatmap comparison of major components of bacteria (A), fungi (B) and virus (C) in HDM from Greer and AirMid by metagenomic analysis.